Year: 2005

Early steps of clathrin-mediated endocytosis involved in phagosomal escape of Fcgamma receptor-targeted adenovirus

Meier, Oliver; Gastaldelli, Michele; Boucke, Karin; Hemmi, Silvio; Greber, Urs F

Early steps of clathrin-mediated endocytosis involved in phagosomal escape of Fcgamma receptor-targeted adenovirus

Abstract

Adenovirus type 2 (Ad2) and Ad5 enter epithelial cells via the coxsackievirus B Ad receptor (CAR) and alpha(v) integrin coreceptors. In the absence of CAR, they can be directed to the Fcgamma receptor 1 of hematopoietic cells by an adaptor comprising the extracellular CAR domain and the Fc portion of a human immunoglobulin G (CARex-Fc). This gives rise to Ad aggregates and single particles which together enhance gene delivery up to 250-fold compared to adaptor-less viruses. A small interfering RNA knockdown of the clathrin heavy chain and quantitative electron microscopy of hematopoietic leukemia cells showed that the majority of Ads were phagocytosed as clusters of 1 to 3 microm in diameter and that about 10% of the particles entered cells by clathrin-mediated endocytosis. The clathrin knockdown did not affect phagocytosis but, surprisingly, inhibited viral escape from phagosomes. Similarly, blocking an early stage of clathrin-coated pit assembly inhibited phagosomal escape and infection but not aggregate uptake, unlike blocking of a late stage of clathrin-coated pit formation. We propose a cooperative interaction of clathrin-mediated endocytosis and phagocytosis triggering phagosomal lysis and infection.

JOURNAL OF VIROLOGY, Feb. 2005, p. 2604–2613 Vol. 79, No. 4
0022-538X/05/$08.00+0 doi:10.1128/JVI.79.4.2604–2613.2005

Early Steps of Clathrin-Mediated Endocytosis Involved in Phagosomal Escape of Fcγ Receptor-Targeted Adenovirus

Oliver Meier,[1] Michele Gastaldelli,[1] Karin Boucke,[1] Silvio Hemmi,[2] and Urs F. Greber[1]*

Zoologisches Institut[1] and Institut für Molekularbiologie,[2] University of Zürich, Zürich, Switzerland

Received 21 August 2004/Accepted 21 September 2004

Adenovirus type 2 (Ad2) and Ad5 enter epithelial cells via the coxsackievirus B Ad receptor (CAR) and α_v integrin coreceptors. In the absence of CAR, they can be directed to the Fcγ receptor 1 of hematopoietic cells by an adaptor comprising the extracellular CAR domain and the Fc portion of a human immunoglobulin G (CARex-Fc). This gives rise to Ad aggregates and single particles which together enhance gene delivery up to 250-fold compared to adaptor-less viruses. A small interfering RNA knockdown of the clathrin heavy chain and quantitative electron microscopy of hematopoietic leukemia cells showed that the majority of Ads were phagocytosed as clusters of 1 to 3 μm in diameter and that about 10% of the particles entered cells by clathrin-mediated endocytosis. The clathrin knockdown did not affect phagocytosis but, surprisingly, inhibited viral escape from phagosomes. Similarly, blocking an early stage of clathrin-coated pit assembly inhibited phagosomal escape and infection but not aggregate uptake, unlike blocking of a late stage of clathrin-coated pit formation. We propose a cooperative interaction of clathrin-mediated endocytosis and phagocytosis triggering phagosomal lysis and infection.

The molecular mechanisms of viral infection through receptor-mediated endocytosis are of increasing interest since they determine the efficacies of natural infections and viral therapies. All known types of endocytosis are used and abused by viruses (reviewed in references 48 and 50). Endocytosis segregates plasma membrane domains into dynamically overlapping internal organelles, allowing both specific and general alterations of the engulfed material (reviewed recently in references 20, 34, and 66). For example, clathrin-mediated endocytosis (CME) rapidly retrieves specific receptors and membranes in all eucaryotic cells. Depending on the receptors, it leads to temporally and spatially controlled internalization and activation or to constitutive uptake and recycling. CME collects transmembrane receptors via the adaptor protein 2 (AP2) and a variety of accessory proteins, including Eps15, amphiphysin, and the large GTPase dynamin (for reviews, see references 8 and 51). In contrast, macropinocytosis and phagocytosis engulf large amounts of membranes, which is important for the uptake of solutes and nutrients and for immune defense. Macropinosomes are induced by actin-driven surface ruffling followed by cell type-specific endosomal maturation steps, including recycling and transport towards tubular lysosomes, as observed in macrophages (25, 31, 41, 45). For many different cell types, macropinocytosis can be triggered by growth factors, viruses, or downstream signaling leading to the closure of lamellipodia at ruffling membranes (for reviews, see references 28, 36, 44, and 55). It is not inhibited by GTPase-defective K44A-dynamin. Growth factors induce macropinosomes which remain largely intact and are shunted into a recycling pathway, whereas adenovirus (Ad)-induced macropinosomes have a propensity to lyse (35). This lysis occurs simultaneously with viral escape from endosomes, suggesting a functional link between macropinocytosis and viral infection.

Fc receptors are key effectors of macropinocytosis in macrophages and dendritic cells. In these cells, macropinosomes are important for major histocompatibility complex class I and class II presentation of exogenous antigens, including viruses and Fcγ receptor (Fcγ-R)-bound ligands (1, 22, 27, 39, 46). In addition, they are involved in phagocytosing large particles during innate and adaptive immune responses through various cell surface receptors, including Fc-Rs. Fcγ-Rs bind immunoglobulin G (IgG) molecules and act as positively or negatively activating multichain receptors (64). The high-affinity human Fcγ-R1 (CD64), for example, binds the Fc portion of IgGs and evokes the phagocytosis of IgG-coated particles (2). Fcγ-R2 (CD32) is a medium-affinity receptor that mainly binds to aggregated IgGs, and Fcγ-R3 (CD16) binds poorly to monomeric IgG and has a low affinity for aggregated IgGs (57, 64). The clustering of macrophage Fcγ-Rs by multimeric Ig complexes then leads to internalization and signaling through immune receptor-based tyrosine motifs, with tyrosine and lipid kinases closing the phagocytic cup (9, 21).

The Fc-R-mediated endocytosis of viruses is physiologically important (23). For example, antibody-loaded Ad type 5 (Ad5) was recently shown to efficiently bind to and internalize in dendritic cells, dependent on Fcγ-R2 and Fcγ-R3 (37). However, it is still unknown how Ad5 transduces dendritic cells, a process thought to be crucial for the activation of CD8-positive T cells commonly observed with therapeutic Ads. For this study, we investigated the transduction mechanism of species C Ad2 and Ad5 targeted to the Fcγ-Rs of THP-1 acute hemocytic leukemia cells by a soluble adaptor of the extracellular domain of the coxsackievirus B Ad receptor (CAR) and the Fc portion of a human IgG (CARex-Fc) (10). THP-1 cells are known to express both the high-affinity Fcγ-R1 and the lower affinity Fcγ-R2, but not Fcγ-R3. Retargeting involves Fcγ-R1, since only anti-CD64 antibodies inhibited Ad5 transduction

* Corresponding author. Mailing address: Zoologisches Institut, University of Zürich, 8057 Zürich, Switzerland. Phone: 41 1 635 4841. Fax: 41 1 635 6822. E-mail: ufgreber@zool.unizh.ch.

and since cells expressing Fcγ-R2 or Fcγ-R3, such as primary NK cells, Raji Burkitt lymphoma cells, and K562 chronic myelogenous leukemia cells, were not transduced with Ad5–CARex-Fc. Our results now reveal that the majority of Ad particles are internalized in THP-1 cells by phagocytosis and that the lysis of Ad-containing phagosomes requires early stages of clathrin-coated pit formation. This is functionally similar to infections of epithelial cells with species C Ads, for which viral uptake and signaling occur through CME and elicit endosomal leakage, lysis of macropinosomes, and infection.

MATERIALS AND METHODS

Cells, viruses, and proteins. Acute monocytic leukemia THP-1 cells were kindly provided by G. Schoedon and P. Peghini, Department of Medicine, University of Zürich. They were cultured in Iscove modified Dulbecco medium plus 10% fetal calf serum. Ad2 and the mutant Ad2 *ts*1 were grown and isolated as described previously (18). [^{35}S]methionine-Ad2 and [^{3}H]thymidine-Ad2 were produced as described previously (19). Ad5-luc and Ad5-eGFP (lacking E1 and E3) expressed luciferase and enhanced green fluorescent protein (eGFP), respectively, from a cytomegalovirus promoter inserted into the E1 region, as described previously (10, 30). CARex-Fc was purified from COS7 cell supernatants and incubated with Ad on ice for 45 min prior to transduction into THP-1 cells as described previously (10). The R72 antibody against fiber was obtained from M. Horwitz (Albert Einstein School of Medicine, New York, N.Y.) and used as previously described (19). The mouse monoclonal antibody OKT-9 against the transferrin receptor (Tfn-R) was prepared from a hybridoma cell line (American Type Culture Collection) by Thomas Ebel (Karolinska Institute, Huddinge, Sweden). A rabbit anti-CRM1 antibody was a kind gift of G. Grosfeld (11). The anti-Fcγ-R1 (31844) and anti-Fcγ-R2 (30934 and 555447) antibodies used for flow cytometry were purchased from BD Biosciences (Basel, Switzerland).

DNAs, siRNAs, and transfections. Dyn2-eGFP and K44A-Dyn2–eGFP expression plasmids were obtained from M. McNiven (Mayo Clinic, Rochester, Minn.) (7), and eGFP-eps15ΔEH2,3 and eGFP-eps15DIIIΔ2 cDNAs were obtained from A. Benmerah (Institut Cochin, Paris, France) (5). eGFP-amphiphysin 1 and eGFP-tagged G684R,P687L (GPRL)-amphiphysin 1 were obtained from P. De Camilli (Yale University School of Medicine, New Haven, Conn.) (15). The hc1 small interfering RNA (siRNA) target sequence was AACCUGC GGUCUGGAGUCAAC (26), the chc2 siRNA sequence was UAAUCCAAU UCGAAGACCAAU (40), and the eGFP siRNA sequence was CGGCAAGC UGACCCUGAAGUUCAU (QIAGEN AG, Basel, Switzerland). Transient transfections of THP-1 cells by nucleofection (by use of Nucleofector T-03, a solution V for Jurkat cells; Amaxa GmbH, Köln, Germany) were carried out in 100-μl volumes containing 2.25×10^6 cells, 1.5 μg of siRNA (QIAGEN AG), or 1.5 μg of plasmid DNA (QIAGEN plasmid maxi kit).

CARex-Fc Ad cluster formation and sucrose density gradients. Ad2 or Ad5 was preincubated with CARex-Fc on ice for 45 min, typically at a ratio of 300 CARex-Fc dimers to each Ad particle, by pipetting up and down once and incubation on ice for 45 min. The mixture was centrifuged through a preparative sucrose gradient consisting of 0.5 ml of 15%, 0.4 ml of 20%, and 0.2 ml of 30% sucrose in 50 mM Tris (pH 7.4)–100 mM NaCl buffer at $8,568 \times g_{max}$ for 25 min. Fractions including the pelleted material were collected from the top, denatured with sodium dodecyl sulfate (SDS; 0.2% final concentration), and mixed with an eightfold excess of Ready-Safe liquid scintillation cocktail (Beckman), and radioactivities were determined with a Beckman LS 3801 scintillation system. The numbers of Ad particles and the amounts of CARex-Fc in preparative sucrose gradients were determined by absorbance intensity quantification of the hexon protein and CARex-Fc monomers by the use of purified Ad2 and CARex-Fc as standards.

Flow cytometry and cell sorting. THP-1 cells were washed with balanced salt solution (0.14 mM NaCl, 1 mM $CaCl_2$, 5.4 mM KCl, 0.8 mM $MgSO_4$, 0.3 mM NaH_2PO_4, and 0.4 mM KH_2PO_4 [pH 6.9]) containing 0.2% fetal calf serum and then were filtered through 50-μm-pore-size Filcons (15047N; Dako, Glostrup, Denmark) at 20 million cells per ml. This allowed a stable flow of 1 million cells per min through a modular flow sorter (Dako Cytomation Bioinstruments GmbH). Using SUMMIT software, we set gates for viable cells, with nonelectroporated cells as a reference. Gates for eGFP-expressing cells were determined by using cells that had been electroporated without DNA. Transfected cells were isolated by fluorescence-activated cell sorter (FACS) gating for viable cells (9 to 19%) and for eGFP expression (11 to 38%). Notably, electroporation alone slightly shifted the peak towards green fluorescence (FL1), which was taken into account when we defined the gate for eGFP expression. Typically, about 15 million cells were used to recover 300,000 cells. Lysates of the sorted cells were subjected to luciferase activity measurements. Dextran-fluorescein isothiocyanate (FITC) uptake into suspended THP-1 cells was measured by FACS analysis as described for KB suspension cells (35).

Electron microscopy. For transmission electron microscopy (TEM), 5×10^5 THP-1 cells were transduced with 300 CARex-Fc dimers per Ad at a multiplicity of transduction (MOT) of 100 at 37°C for 60 min after cold synchronization. This corresponded to 5 μg of Ad and 1.2 μg of CARex-Fc. The cells were fixed in 1.5% glutaraldehyde–2% formaldehyde in 0.1 M cacodylate buffer (pH 7.4) for 60 min in an Eppendorf tube at room temperature. The cells were washed by centrifugation at $3,300 \times g$ in a tabletop Eppendorf centrifuge, postfixed in 1.5% potassium ferricyanide–1% OsO_4 in double-distilled water (ddH_2O) at 4°C for 60 min, washed, prestained with 1% tannic acid in 0.05 M cacodylate buffer for 45 min, washed twice with 1% sodium sulfate in 0.05 M cacodylate buffer, washed with ddH_2O, prestained in 2% uranyl acetate in ddH_2O for 60 min, and finally washed in ddH_2O (53). The cells were dehydrated stepwise in ddH_2O-acetone, embedded in Epon, and collected by centrifugation at $9,300 \times g$ for 2 min. The Epon-embedded cells were kept at 60°C for 3 days to polymerize the medium. Thin sections were cut on a Leica-Ultracut stage and were observed with a Zeiss EM 902A microscope. Statistical analyses of TEM were performed as described previously (43). EM analysis of Tfn-R internalization was performed as described above for virus-infected cells. THP-1 cells (5×10^5) were incubated in Hanks medium containing 0.2% bovine serum albumin (BSA) in the cold with a monoclonal antibody directed against human Tfn-R at a dilution of 1:100 for 45 min. The cells were washed twice by centrifugation at $190 \times g$ and then incubated with a secondary goat anti-mouse IgG coupled to 5-nm-diameter gold particles (2 μg/ml). The cells were washed twice, suspended in 500 μl of warm Hanks medium–0.2% BSA, and incubated in an orbital reaction tube shaker (Eppendorf; speed setting 10) at 37°C for 30 min. The cells were pelleted by centrifugation, suspended in EM fixative, and processed for TEM as described above.

RESULTS

CARex-Fc Ad clusters bind and transduce THP-1 cells. Hematopoietic cells are difficult to transduce with species C Ad vectors because they express low levels of the cell surface proteins CAR and α_v integrins (42). CARex-Fc adaptors, however, mediate viral binding to hematopoietic cells with up to 250-fold enhanced transduction rates (10). In nonreducing SDS-polyacrylamide gel electrophoresis (SDS-PAGE), the CARex-Fc protein runs as a dimer, consistent with the dimeric nature of IgGs (64) and the extracellular domain of CAR (58). We first analyzed the binding to THP-1 cells of [^{35}S]methionine-labeled Ad2 that had been preincubated with different amounts of CARex-Fc. Ad2 binding depended on the dose of CARex-Fc, with optimal binding at ratios of about 120 to 600 CARex-Fc dimers to each Ad particle (Fig. 1A), consistent with an optimal ratio of about 300 CARex-Fc dimers to each Ad particle (10). An EM analysis of negatively stained Ad2 incubated with a 300-fold molar excess of CARex-Fc directly visualized viral aggregates with a typical cluster size of 30 to 50 particles and ranging up to 100 particles, with diameters ranging from one to several micrometers (Fig. 1B). In addition, a small number of single particles was detected, comparable to purified Ad2 without CARex-Fc. We next analyzed the CARex-Fc-coated Ads in sucrose velocity gradients. Different amounts of CARex-Fc were incubated with radiolabeled Ad2, centrifuged through sucrose, fractionated, and analyzed by liquid scintillation counting. At 300 CARex-Fc dimers per Ad particle, about 30% of the particles were recovered in fractions that were denser than Ad2 alone (Fig. 2A, fractions 9 and 10 and pellet). Ratios of CARex-Fc to Ad2 as low as 3 still gave rise to aggregates, whereas a large excess of 6,000 CARex-Fc dimers per Ad2 particle did not lead to aggregates, indicating

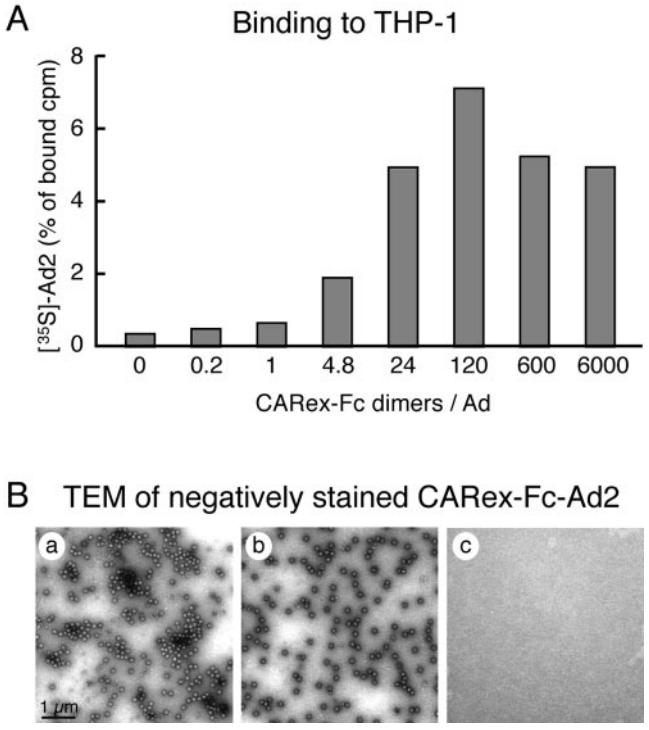

FIG. 1. Dose-dependent binding of CARex-Fc–Ad2 clusters to THP-1 cells. (A) [^{35}S]methionine-labeled Ad2 (2.5×10^9 particles, 81,000 cpm) was incubated with different amounts of CARex-Fc in 20 μl of ice-cold phosphate-buffered saline for 45 min, added to 5×10^5 THP-1 cells in 0.5 ml of cold RPMI containing 0.2% BSA, and incubated in the cold on a rocking platform for 60 min. The cells were washed twice in cold RPMI-BSA and resuspended in 0.2% SDS, and the amount of cell-associated Ad2 was determined by scintillation counting. Results are expressed as percentages of bound Ad2. (B) Ad2 (1.68 μg) was incubated with (a) or without (b) CARex-Fc (0.43 μg) in 13 μl of PBS on ice for 45 min, spotted on an EM grid, negatively stained with uranyl acetate, and observed by TEM (×12,000). CARex-Fc alone (0.43 μg in 13 μl) is shown in panel c. Bar = 1 μm.

that saturation had occurred (not shown). SDS-PAGE analyses of sucrose velocity gradients indicated that aggregates of 300 CARex-Fc dimers per Ad contained about 200 CARex-Fc dimers associated with each virus particle (Fig. 2B). This was about sixfold more than expected, assuming that 12 trimeric fibers per Ad would each bind three CARex-Fc dimers. Whether these large amounts of CARex-Fc in the viral aggregates were due to the small fraction of trimeric CARex-Fc adaptor, detected by its apparent molecular mass of about 170 kDa, is unknown. In contrast, particles recovered from the middle of the gradient and forming bands at the same locations as untreated particles (Fig. 2A) contained 10 to 20 CARex-Fc dimers per Ad, that is, single particles whose fibers were all coated with at least one adaptor (Fig. 2B). Above these fractions, the loading zone of the gradient was highly enriched with free CARex-Fc. In transduction experiments with THP-1 cells, the isolated aggregates or a mixture of aggregates and free Ad5-luc was three- to fourfold more effective than single Ads recovered from the middle of the gradient on a per virus basis (Fig. 2B, fractions 5 and 6, and Fig. 2C). These results are consistent with the notion that monomeric CARex-Fc adaptors are 50 to 100 times less efficient than the dimeric CARex-Fc

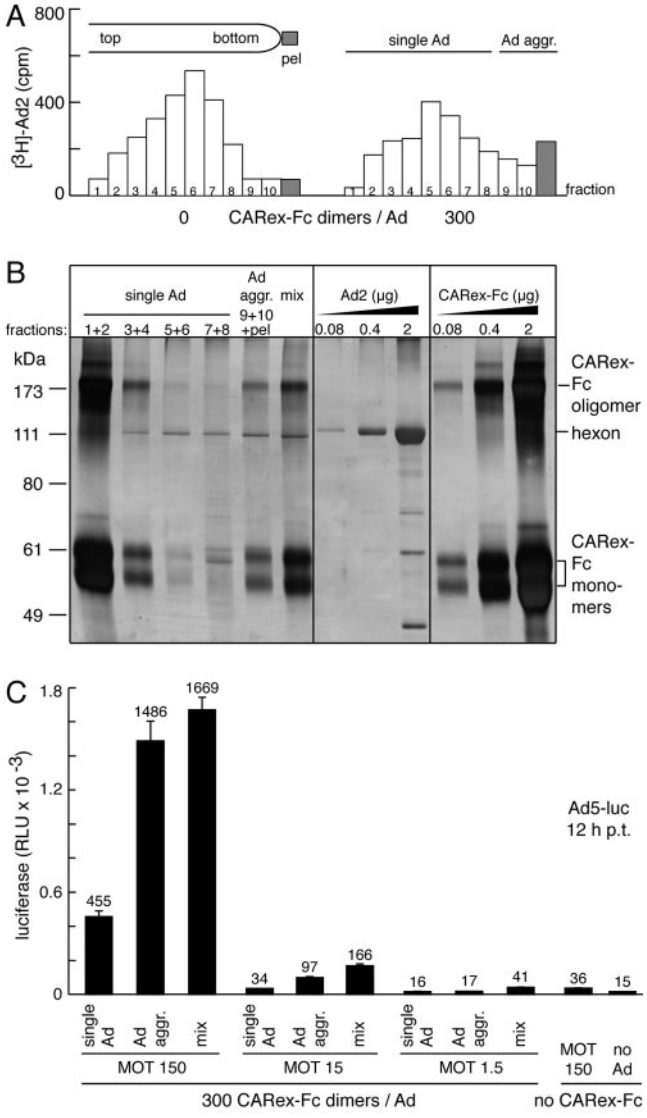

FIG. 2. Isolated CARex-Fc–Ad5 clusters transduce THP-1 cells. (A) Ad5-luc (120 μg) containing 1.7% [^{3}H]Ad2 (38,000 cpm) was preincubated with 32 μg of either BSA or CARex-Fc on ice for 45 min (0 and 300 CARex-Fc dimers per Ad particle, respectively), loaded on a sucrose step gradient (0.5 ml of 15%, 0.4 ml of 20%, and 0.2 ml of 30% sucrose), and centrifuged at 8,570 × *g* for 25 min, and the amount of ^{3}H in each fraction was determined by scintillation counting. (B) Aliquots of combined sucrose gradient fractions (1.4% of each) and an aliquot of the total material loaded on the gradient (mix) were precipitated with trichloroacetic acid, dissolved in partly reducing SDS sample buffer, and analyzed in a 10% polyacrylamide–SDS gel, which was then stained with silver as described previously (24). Standards of Ad2 and CARex-Fc ranging from 0.08 to 2 μg are shown on the right side. The Ad hexon protein was detected at 111 kDa. CARex-Fc oligomers ran at 180 kDa, and two differentially glycosylated forms of CARex-Fc monomers ran at 60 and 55 kDa (10). (C) Equal amounts of isolated single particles (fractions 5 and 6), viral aggregates (fractions 9 and 10 and the pellet), and the nonfractionated mixture of Ad5-luc and CARex-Fc (mix) were added to 10^5 THP-1 cells at MOTs of 150, 15, and 1.5. The luciferase activity was determined at 12 h posttransduction, as indicated by the means of three parallel samples in relative light units (RLU) normalized to the cell numbers, including standard errors of the means (SEM).

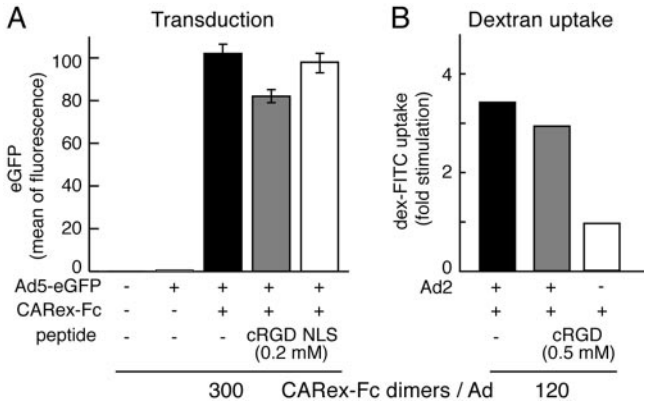

FIG. 3. CARex-Fc–Ad-induced transduction and endocytosis of THP-1 cells are largely independent of cRGD peptides. (A) THP-1 cells (5×10^5 in 0.5 ml) expressing very low levels of α_v integrins (42) were preincubated with or without 0.2 mM cRGD or 0.2 mM NLS control peptides for 30 min at 37°C, followed by incubation with Ad5-eGFP CARex-Fc mixtures (0.9 μg of Ad5; 300 dimers/Ad particle) for 60 min in the cold. Under these conditions, about 5% of the input virus was bound, corresponding to an MOT of 35. The cells were washed and incubated in warm medium for 24 h and then subjected to flow cytometry for eGFP measurements. The means of three independent experiments are shown, including standard deviations. (B) THP-1 cells (5×10^5) pretreated with or without 0.5 mM cRGD peptides were incubated with Ad2 (13.5 μg) that had been preloaded with CARex-Fc at a ratio of 120 dimers/Ad particle in the cold for 60 min (MOT = 300). The cells were washed, warmed at 37°C for 5 min, pulsed with dextran-FITC (1 mg/ml) at 37°C for 5 min, and analyzed by flow cytometry. The results are expressed as levels of stimulation of dextran uptake compared to uninfected cells. Results for one of three representative experiments are shown.

adaptor at transducing THP-1 cells (data not shown). Furthermore, CARex-Fc-mediated transduction was not sensitive to the integrin inhibitor cyclic arginine-glycine-aspartate (cRGD) (Fig. 3A), which blocks Ad2 entry into epithelial cells (18, 62). Likewise, cRGD did not significantly inhibit the stimulation of fluid-phase uptake of dextran-FITC, as measured by flow cytometry, suggesting that RGD-binding integrins, such as α_v integrins, were not involved in Fcγ-R-mediated transduction (Fig. 3B). We concluded that a mixture of single Ads and Ad aggregates in association with CARex-Fc adaptors effectively transduced THP-1 cells and strongly enhanced the uptake of fluid-phase material.

Phagocytosis of Ad–CARex-Fc clusters. The stimulation of fluid-phase endocytosis by CARex-Fc was also observed with the Ad2 mutant *ts*1, although it was not as pronounced as that with wild-type Ad2 (Fig. 4A and C). In epithelial cells, *ts*1 fails to escape from endosomes due to an unprocessed capsid structure (17). The dextran-FITC uptake peaked at 30 to 300 CARex-Fc dimers per Ad particle, and stimulation declined at the high ratio of 6,000 CARex-Fc dimers per Ad, consistent with the lack of aggregates and with viral delivery to the cytosol (not shown). Quantitative EM analyses indicated that at 300 CARex-Fc dimers per Ad, 57% of the cell-associated Ad2 particles were present in the cytosol and 15% were present at the nuclear membrane (Fig. 4B). The rest were equally distributed at the plasma membrane and in endosomal vesicles, including phagosomes. Clusters of 30 CARex-Fc dimers per *ts*1 particle were also efficiently phagocytosed and released into the cytosol, albeit with a somewhat lower efficiency than that for Ad2 particles (Fig. 4D). The same result was obtained with 300 CARex-Fc dimers per *ts*1 particle (not shown), suggesting that the nature of the capsid also contributes to viral escape from endosomes. Interestingly, Fcγ-R-targeted *ts*1 aggregates escaped more efficiently from THP-1 phagosomes than *ts*1 particles from HeLa cell endosomes ($P = 0.05$), indicating that Fcγ-R ligation contributes to viral escape. We concluded that CARex-Fc-formed clusters of Ad and *ts*1 bind to Fcγ-R-positive THP-1 cells, are internalized by phagocytosis, and give rise to the majority of cytosolic Ad particles.

Clathrin is required for escape of Fcγ-R-targeted Ad from phagosomes. Earlier observations suggested that impairing the function of clathrin (49), dynamin 2 (14), or amphiphysin 2 (13) depressed the phagocytic efficiency of cells. A recent report, however, showed that the inhibition of dynamin or the reduction of clathrin by the expression of antisense mRNA had no effects on the formation of phagosomes in mouse RAW-264.7 macrophages (56). We investigated the requirement of clathrin for the phagocytosis of CARex-Fc Ad clusters, taking advantage of recent reports showing a functional knockdown of the clathrin heavy chain (CHC) by siRNAs in epithelial cells (26, 40). THP-1 cells were transfected by nucleofection with siRNAs against CHC (hc1 [26] and chc2 [40]) or with a siRNA against eGFP as a control. Cells were transfected again after 2 days and were transduced on day 4 with CARex-Fc Ad5-luc aggregates (300:1) for 24 h. The abundance of CHC was assessed by Western blotting 0 and 24 h after transduction (Fig. 5A). The hc1 siRNA reduced the levels of CHC to 25 and 13% at 0 and 24 h posttransduction, respectively, and the chc2 siRNA reduced the levels to 43 and 31%, respectively, of control cell levels. In contrast, the siRNA against eGFP gave 108 and 80% of the control clathrin levels, normalized to the amounts of the 58-kDa protein band in parallel silver-stained SDS gels or to the amounts of CRM1 on the same nitrocellulose filter. Cell treatment with the hc1 siRNA reduced the levels of luciferase expression about 50%, and the chc2 siRNA treatment reduced the levels about 20% compared to those in eGFP siRNA-treated cells (Fig. 5B). These inhibitions were not due to decreased levels of cell surface Fcγ-R1 or to reduced cell viability, as determined by flow cytometry (data not shown). A TEM analysis indicated that >54% of the Ads were in endosomal or phagosomal structures of hc1 siRNA-treated cells, whereas only 33% of the Ads were enclosed by membranes in eGFP control siRNA-treated cells or cells that were not treated with siRNA at 60 min postinfection (Fig. 5C). In eGFP siRNA-treated cells and non-siRNA control cells, virus particles were often found in cytosolic clusters without a limiting membrane. In hc1 siRNA-treated cells, the amount of cytosolic Ads was reduced to 30% of the total cell-associated virus, in contrast to about 60% in either type of control cells. The amounts of cell surface Ads were significantly increased, from 5 to 16% ($P = 0.025$), suggesting that a small fraction of Ad particles enter by CME. This indicated that clathrin is required for phagosomal escape but not for the phagocytic uptake of Ad.

Fcγ-R-mediated transduction of THP-1 cells requires early stages of clathrin-mediated endocytosis. CME can be inhibited by overexpressing a dominant-negative Eps15 protein which tightly binds to the alpha subunit of AP2 (5) and thereby

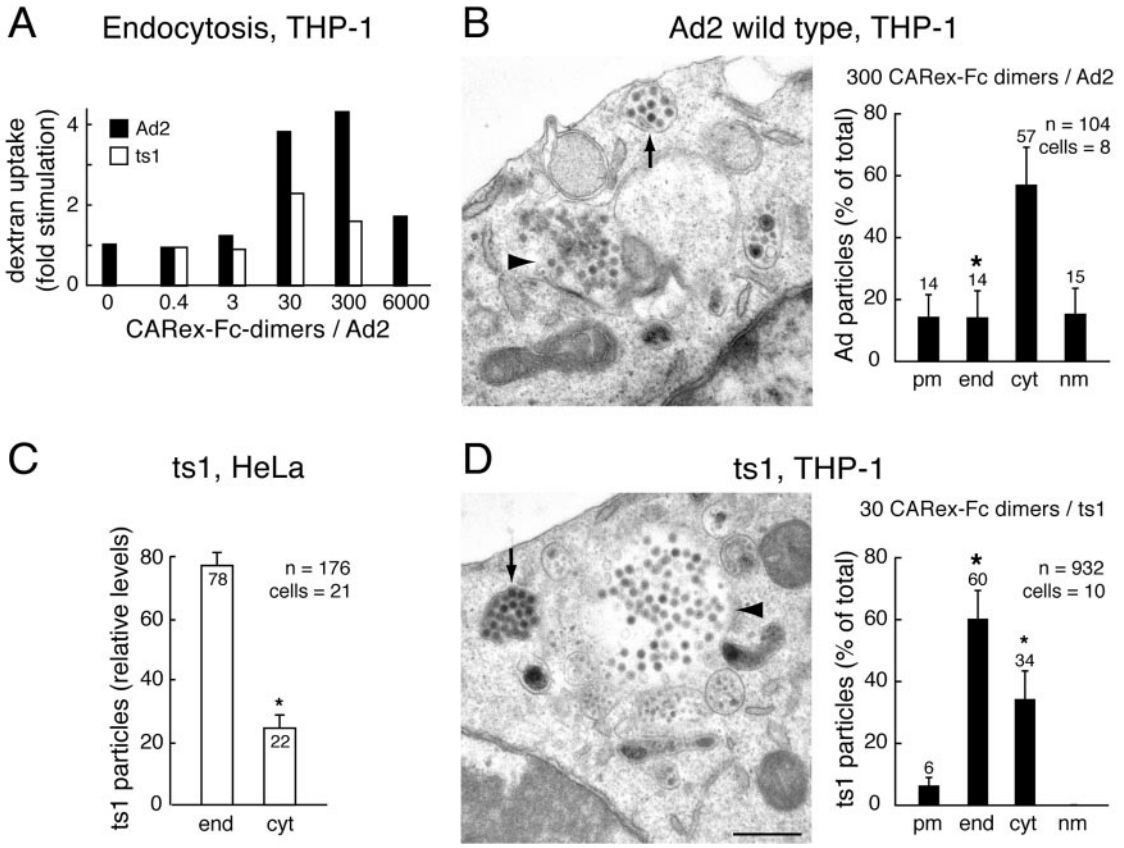

FIG. 4. Clusters of CARex-Fc–Ad2 and *ts*1 are phagocytosed and released into THP-1 cells. (A) CARex-Fc dose-dependent stimulation of fluid-phase uptake by Fcγ-R-targeted Ad2 and *ts*1. THP-1 cells (5×10^5) were incubated with different ratios of preincubated CARex-Fc dimers to Ad2 (8 μg) in the cold for 60 min, washed, warmed for 5 min, pulsed with dextran-FITC for 5 min, harvested, and analyzed by FACS. Results are expressed as levels of stimulation of dextran uptake compared with uninfected cells. The experiment was performed twice with similar results. (B and D) Ad2 (B) and *ts*1 (D) in complex with CARex-Fc are delivered to the THP-1 cytosol. Ad2 and *ts*1 were incubated with 300 and 30 CARex-Fc dimers/particle, respectively, and then incubated with THP-1 cells at an MOT of 100 for 1 h in the cold. The cells were washed, warmed for 60 min, fixed, and processed for TEM. Arrows indicate endosomal virus aggregates, and arrowheads depict cytoplasmic virus particles. Bar = 500 nm. The numbers of virus particles at the plasma membrane (pm), endosomes (end), cytosol (cyt), and the nuclear membrane (nm) were quantified. Mean values derived from the indicated numbers of cells are expressed as percentages of total virus particles with corresponding SEM. *n*, number of Ad particles. The large asterisks indicate differences between endosomal Ad2 and endosomal *ts*1 with *P* values of <0.01 in one-sided *t* tests. The small asterisk indicates a difference in the cytosolic localization of *ts*1 in HeLa cells with a *P* value of 0.05 (C). The *P* values of the other *ts*1 compartments in comparison with Ad2 in THP-1 and *ts*1 in HeLa cells were >0.05, i.e., the differences are not significant. (C) *ts*1 predominantly localizes to endosomes of HeLa cells in the absence of CARex-Fc. HeLa cells expressing CAR and α_v integrins were infected with *ts*1 for 60 min upon cold binding of virus, fixed, and processed for TEM. The subcellular distribution of virus particles was quantified. Less than 10% of the virus particles were at the plasma membrane, and none were found at the nuclear membrane (not shown).

inhibits the recruitment of NPF-motif-carrying accessory proteins such as synaptojanin, epsin, and AP180 (8). This blocks the formation of clathrin-coated vesicles at an early stage, that is, it results in flat clathrin-coated membrane lattices. At a later stage of CME, amphiphysin interacts with dynamin and synaptojanin via its C-terminal SH3 domain. The G684R,P687L (GPRL)-amphiphysin 1 mutant with a defective SH3 domain does not interact with dynamin and synaptojanin and inhibits CME at a late stage of clathrin-coated pit assembly (52, 54). We tested whether the disruption of CME by dominant-negative eGFP-tagged Eps15ΔEH2,3 and eGFP–GPRL-amphiphysin would affect the transduction of Ad5-luc–CARex-Fc clusters. Nucleofected THP1 cells were transduced with Ad5-luc for 24 h, isolated by FACS based on eGFP expression, and analyzed for luciferase expression (Fig. 6A). eGFP-Eps15ΔEH2,3 inhibited luciferase expression about 80% (Fig. 6B), similar to dominant-negative K44A-Dyn2–eGFP, which interfered with the phagocytic uptake of Ad5 clusters (not shown). Strikingly, eGFP–GPRL-amphiphysin1 only slightly (about 15%) inhibited the expression of luciferase compared to control transfections. eGFP-Eps15ΔAP2, which does not bind to AP2α, and eGFP-tagged wild-type amphiphysin 1 had no effects on luciferase expression. We assessed the effects of eGFP-Eps15ΔEH2,3 and eGFP–GPRL-amphiphysin1 on Tfn-R endocytosis in THP-1 cells by pre-embedding immuno-EM at 30 min postinternalization, using an anti-Tfn-R monoclonal antibody and a secondary anti-mouse IgG tagged with 5-nm-diameter colloidal gold in the absence of virus. In control cells and Eps15ΔAP2- and wild-type amphiphysin 1-expressing cells, gold particles indicative of Tfn-R were found on endosomal membranes and on the plasma membrane (Fig. 7). Cells expressing eGFP-Eps15ΔEH2,3 or

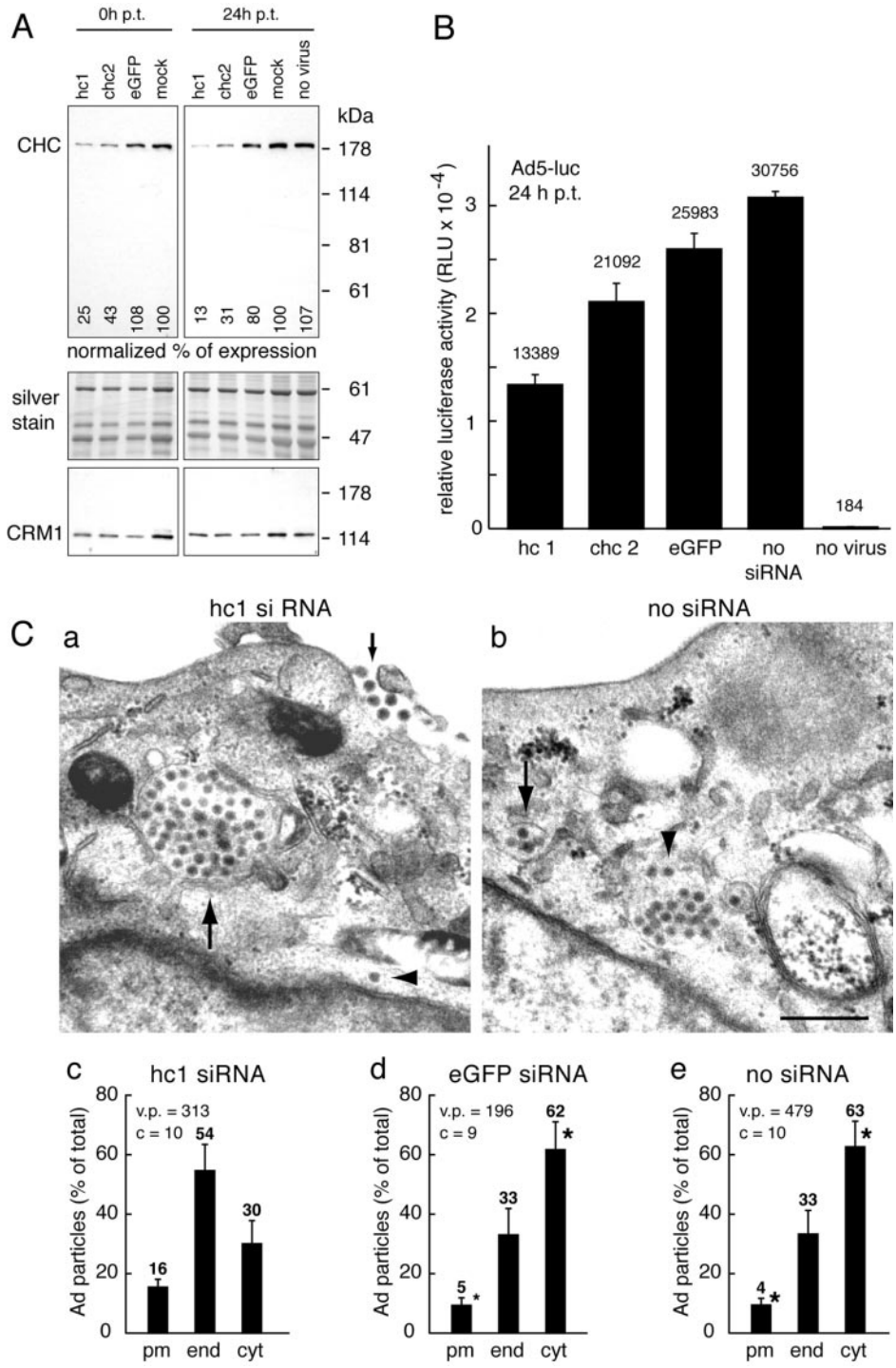

FIG. 5. Clathrin is required for escape of Fcγ-R-targeted Ad from phagosomes. (A) THP-1 cells (2×10^6) were doubly transfected by nucleofection with hc1 and chc2 siRNAs against CHC and with a siRNA against eGFP with a 48-h interval and then were transduced with Ad5-luc. On day 4 after the initial nucleofection, i.e., at 0 h posttransduction (p.t.) and also at 24 h p.t., 2×10^5 cells were analyzed by SDS–7.5% PAGE, silver staining, and Western blotting with antibodies against CHC and the nuclear export factor CRM1 as a control. The levels of CHC after normalization to the amount of untransfected cells (mock) and loaded protein are indicated. (B) Transfected and untransfected THP-1 cells (4×10^5) were transduced with 300 CARex-Fc dimers per Ad at an MOT of 20 for 24 h, and luciferase activities were determined for half of the cells. The means of three measurements normalized to the amounts of protein in the samples are indicated, including SEM. The other half of the samples were subjected to SDS-PAGE (see panel A). Similar results were found for another independent experiment. (C) TEM analyses of incoming Ad2 at 60 min p.t. in clathrin siRNA (a)- and control (b)-transfected THP-1 cells. Arrowheads depict cytoplasmic virus, and arrows show particles in endosomes. Bar = 500 nm. The amounts of virus particles at the plasma membrane (pm), in endosomes (end), and in the cytosol (cyt) were quantified. The mean values and corresponding SEM based on the numbers of cells and virus particles analyzed (c and v.p., respectively) are expressed as percentages of total virus particles. The large asterisks indicate differences ($P < 0.01$ by one-sided t tests) between cytosolic and plasma membrane Ad2 in eGFP siRNA- and non-siRNA-treated cells compared to the corresponding locations of Ad in hc1 siRNA-treated cells. The small asterisk indicates a difference with a P value of 0.025.

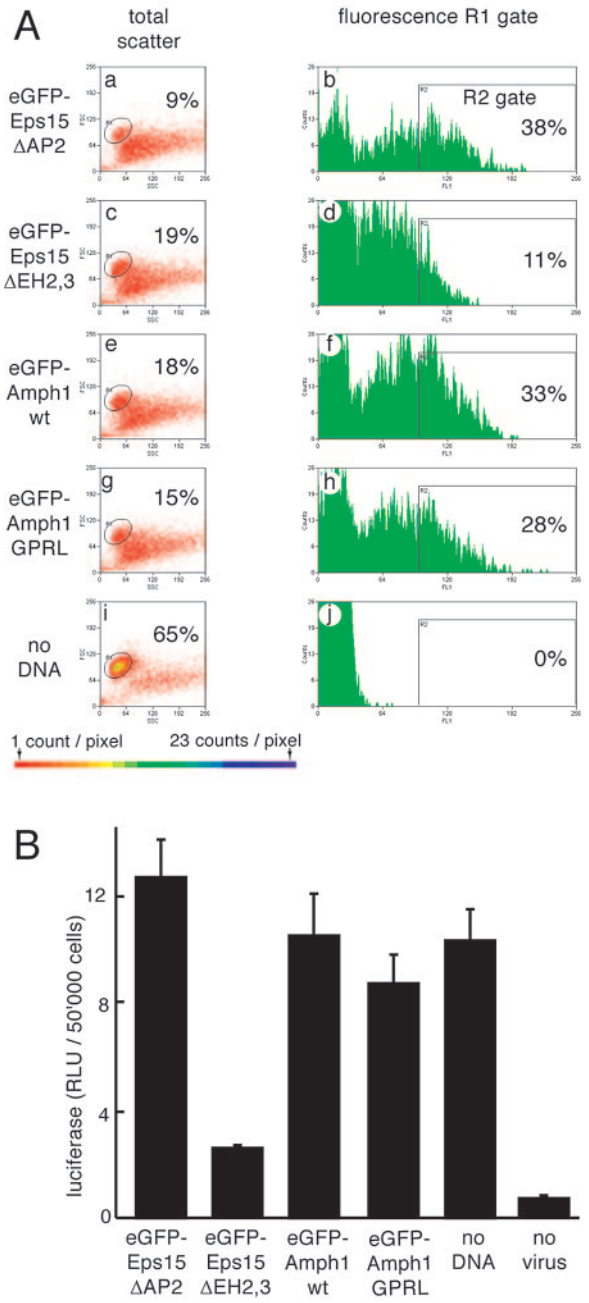

FIG. 6. Early steps of clathrin-mediated endocytosis are required for transduction of Fcγ-R-targeted Ad. (A) THP-1 cells (15×10^6) were transfected by nucleofection with eGFP-Eps15ΔAP2 (a, b), eGFP-Eps15ΔEH2,3 (c, d), eGFP-Amph1 wt (e, f), eGFP–Amph1-GPRL (g, h), or no DNA (i, j) for 24 h. The cells were then transduced with 300 CARex-Fc dimers per Ad5-luc particle at an MOT of 100 for 24 h. From the viable cells (circled in panels a, c, e, g, and i and displayed in the fluorescence R1 gate), the eGFP-positive cells were isolated by FACS (R2 gate) and are indicated as percentages of gated cells. A color scale of the cell counts is also indicated, with each step from red to blue representing one count more per pixel. FSC, forward scatter; SSC, side scatter; FL1, eGFP fluorescence. (B) The eGFP-sorted cells from panel A were subjected to luciferase assays, and the results indicate the means of three measurements (relative light units) normalized to the number of sorted cells, including SEM.

eGFP–GPRL-amphiphysin1 internalized significantly less Tfn-R, amounting to 16 and 11%, respectively, in contrast to 53 and 44% of the control cells ($P < 0.01$ and $P = 0.025$, respectively). Together, these data show that early stages of CME are required for both the phagosomal escape and transduction of THP-1 cells by Fcγ-R-targeted Ad clusters and also for the uptake of presumably single Ad particles. The former delivers the bulk mass of Ad particles into the cell, and the latter delivers a small number of particles. In contrast, blocking the late stages of CME inhibited clathrin-dependent viral uptake but not the phagocytic uptake of Ad clusters or the phagosomal escape and transduction of THP-1 cells.

DISCUSSION

Viruses have evolved to utilize and modify a variety of endocytic uptake mechanisms for cell entry and regulation. The viral choice of a particular entry pathway is based on the availability of primary and secondary receptors, the kinetics and capacity of the endocytic processes, and the subcellular routing of the engulfed material. Normally, a virus strain enters a host cell by a few predominant pathways. When the predominant pathway is blocked or not available, alternative entry gates are used, but these are usually less efficient and may lead to attenuated infections. Many experiments which retargeted viruses from their native receptors to alternative receptors have shown that cell surface attachment is often insufficient for sustained viral entry and gene expression (for reviews, see references 29, 32, and 61). For example, the targeting of Ad to the CD21 or CD34 receptors of hematopoietic cells or the Tfn-R of brain microcapillary endothelial cells yielded virus binding to the target cells, but transgene delivery was low (65).

For this study, we targeted Ad to the high-affinity Fcγ-R1 (CD64) of hematopoietic leukemia cells lacking CAR and essential α_v integrins through a bispecific soluble adaptor, CARex-Fc. This strategy may be of general importance for clinical applications of both lytic and therapeutic transgene-bearing viruses, since CD64 is expressed on subtypes of acute myeloid leukemia (AML) cells, monocytes, and macrophages but not on mature dendritic cells. Notably, the survival rates for AML patients treated with conventional therapies are low (4). AML cells are particularly accessible for gene therapy since the techniques for bone marrow and blood cell transplantations are well established and, importantly, transductions can be performed ex vivo.

Our analyses of ex vivo transduction mechanisms suggested a cooperative involvement of two distinct endocytic pathways, the phagocytic uptake of large clusters of viruses and early stages of clathrin-mediated uptake of single particles. Phagocytosis is responsible for the internalization of the bulk mass of Ad–CARex-Fc clusters, while the clathrin pathway is involved in breaking open the limiting phagosomal membrane and delivering infectious endocytic virus particles to the cytosol. Importantly, the clathrin pathway was not involved in the phagocytic uptake of Ad clusters, e.g., by recycling membranes to phagosomal cups. Breaking of the phagosomal membrane was found to be inhibited in clathrin knockdown cells or cells expressing a dominant-negative accessory protein of CME, Eps15 lacking two of its three EH domains. In addition, isolated viral clusters were fully efficient only if they also con-

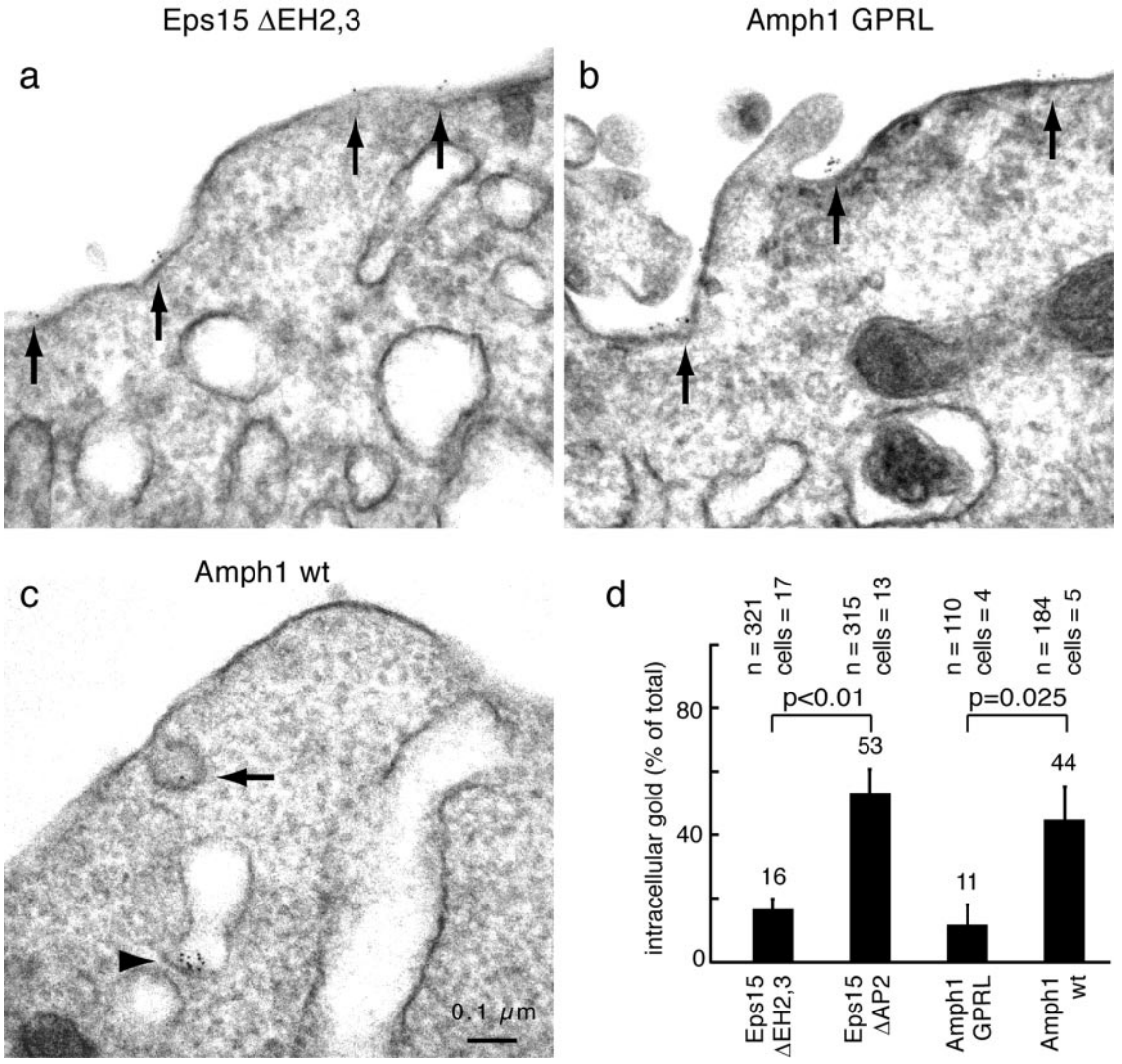

FIG. 7. eGFP-Eps15ΔEH2,3 and eGFP–GPRL-amphiphysin1 block transferrin uptake in THP-1 cells. THP-1 cells (15×10^6) were transfected by nucleofection with eGFP-tagged plasmids encoding Eps15ΔEH2,3, Eps15ΔAP2, amphiphysin 1 (Amph1), and Amph1-GPRL for 24 h. The eGFP-sorted cells were starved of serum in Dulbecco modified Eagle medium-BSA for 4 h, incubated in the cold with mouse anti-transferrin receptor monoclonal antibodies and anti-mouse IgG coupled to 5-nm-diameter colloidal gold, warmed for 30 min, and processed for TEM (for the complete experiment, also see Fig. 6 and its legend). The numbers of gold particles on the plasma membrane (arrows) and on endosomal membranes (arrowhead in panel c) were determined, and the amounts of endosomal gold represented in panel d are percentages of the total, including the number of gold particles (*n*) and the number of cells analyzed.

tained single Ad particles coated with CARex-Fc, supporting the notion that CME is directly rather than indirectly required for phagosomal lysis. Both clathrin and Eps15 are involved in early steps of the formation of clathrin-coated vesicles. Eps15 binds to the clathrin adaptor AP180 and thereby stimulates the formation of clathrin-coated membrane domains. These interactions occur between the EH domains of Eps15 and the NPF motifs of AP180 (33, 38). Intriguingly, dominant-negative GPRL-amphiphysin1 did not affect the efficacy of Fcγ-R1-mediated Ad5 transduction. GPRL-amphiphysin1 has a defective SH3 domain and does not interact with dynamin, thus blocking CME at the step of invaginated coated pits (15, 47). This was verified by measurements of Tfn-R uptake in transfected THP-1 cells. Therefore, the formation of late but not early stages of clathrin-coated pits without vesicle detachment from the plasma membrane gives rise to the full potency of phagocytic transduction via the Fcγ-R.

We propose that clathrin-coated pits serve as a signaling platform from which a virus can induce phagosomal lysis. This is consistent with the notions that Fcε-R1 and Fcγ-R2A internalize small clusters of ligands by CME and that CME-associated Fcε-R1 engages discrete signaling complexes while larger clusters of ligands are engulfed by phagocytosis (6, 63). Our CARex-Fc–Ad clusters are considered to be of a medium to large size (1 to 3 μm), but they also contain small amounts of single virus particles coated with the adaptor. It is possible that single Ad particles engage Fcγ-R1 or Fcγ-R2A, thus inducing CME. Notably, antibodies against Fcγ-R2 did not inhibit the transduction of CARex-Fc–Ad clusters in THP-1 cells (not shown), whereas anti-Fcγ-R1 antibodies had a strong blocking

effect (10). Given that the spatial relationship between CME and phagocytic cups is unknown, Ad-bearing clathrin-coated pits may be formed on the phagosomal membrane or on the nearby plasma membrane (3, 56). It is possible that CME of Ad particles occurs on the phagosomal membrane and there induces disruption of the phagosome. Since the plasma membrane is not disrupted in Ad-infected cells, this scenario would require a differential mechanism for CME on the phagosomal membrane versus that on the plasma membrane. Interestingly, it has been suggested for mouse RAW-264.7 macrophages that Tfn-R endocytosis from phagosomal membranes is independent of K44A-dynamin, unlike Tfn-R endocytosis from the plasma membrane (56).

Alternatively, Ad particles in clathrin-coated pits of the plasma membrane may elicit signals that are received by the phagosomes and that trigger phagosomal lysis. We have analyzed this possibility by using epithelial cells, in which Ad2 entry by CME was blocked by dominant-negative forms of CHC, Eps15, or the GTPase-defective K44A-dynamin (35, 36, 59). Coincident with viral entry, macropinocytosis is stimulated and macropinosomes are lysed within a few minutes after their formation. Although viruses are found on macropinosomal membranes, they are not sufficient for macropinosomal lysis (35). We suggest that additional factors comprising signals from the cell surface contribute to macropinosomal and phagosomal lysis. While the lysis of macropinosomes in epithelial cells requires both CAR and α_v integrins, the lysis of phagosomes by Ad–CARex-Fc is independent of α_v integrins, suggesting that ligation to Fcγ-R1 sufficiently activates the cell. Indeed, Fcγ-Rs engaged in endocytic processes signal through the small G proteins Rac and Cdc42, through phosphatidylinositol-3-kinase, and through protein kinase C (2, 12, 60), which is strikingly similar to the case for incoming Ad in epithelial cells (16). This signaling, together with the contribution of the virus particles themselves, is required for phagosomal lysis.

ACKNOWLEDGMENTS

We thank Eva Niederer (Institut für Biomedizinische Technik, ETH, Zürich, Switzerland) for help with FACS analyses; Alex Benmerah, Pietro Di Camilli, Harvey McMahon, and Mark McNiven for DNA constructs; and the members of the Greber lab for discussions.

Financial support was obtained from the Cancer League of the Kanton Zürich, the Swiss National Science Foundation, the Kanton Zürich (UFG), and the Julius Müller Stiftung (S.H.).

REFERENCES

1. **Ackerman, A. L., C. Kyritsis, R. Tampe, and P. Cresswell.** 2003. Early phagosomes in dendritic cells form a cellular compartment sufficient for cross presentation of exogenous antigens. Proc. Natl. Acad. Sci. USA **100:** 12889–12894.
2. **Aderem, A., and D. M. Underhill.** 1999. Mechanisms of phagocytosis in macrophages. Annu. Rev. Immunol. **17:**593–623.
3. **Aggeler, J., and Z. Werb.** 1982. Initial events during phagocytosis by macrophages viewed from outside and inside the cell: membrane-particle interactions and clathrin. J. Cell Biol. **94:**613–623.
4. **Arceci, R. J.** 1998. The potential for antitumor vaccination in acute myelogenous leukemia. J. Mol. Med. **76:**80–93.
5. **Benmerah, A., M. Bayrou, N. Cerf-Bensussan, and A. Dautry-Varsat.** 1999. Inhibition of clathrin-coated pit assembly by an Eps15 mutant. J. Cell Sci. **112:**1303–1311.
6. **Booth, J. W., M. K. Kim, A. Jankowski, A. D. Schreiber, and S. Grinstein.** 2002. Contrasting requirements for ubiquitylation during Fc receptor-mediated endocytosis and phagocytosis. EMBO J. **21:**251–258.
7. **Cao, H., F. Garcia, and M. A. McNiven.** 1998. Differential distribution of dynamin isoforms in mammalian cells. Mol. Biol. Cell **9:**2595–2609.
8. **Conner, S. D., and S. L. Schmid.** 2003. Regulated portals of entry into the cell. Nature **422:**37–44.
9. **Crowley, M. T., P. S. Costello, C. J. Fitzer-Attas, M. Turner, F. Meng, C. Lowell, V. L. Tybulewicz, and A. L. DeFranco.** 1997. A critical role for Syk in signal transduction and phagocytosis mediated by Fcgamma receptors on macrophages. J. Exp. Med. **186:**1027–1039.
10. **Ebbinghaus, C., A. Al-Jaibaji, E. Operschall, A. Schoeffel, I. Peter, U. F. Greber, and S. Hemmi.** 2001. Functional and selective targeting of adenovirus to high affinity Fcγ receptor I-positive cells using a bispecific hybrid adaptor. J. Virol. **75:**480–489.
11. **Fornerod, M., J. van Deursen, S. van Baal, A. Reynolds, D. Davis, K. G. Murti, J. Fransen, and G. Grosveld.** 1997. The human homologue of yeast CRM1 is in a dynamic subcomplex with CAN/Nup214 and a novel nuclear pore component Nup88. EMBO J. **16:**807–816.
12. **Garrett, W. S., L. M. Chen, R. Kroschewski, M. Ebersold, S. Turley, S. Trombetta, J. E. Galan, and I. Mellman.** 2000. Developmental control of endocytosis in dendritic cells by Cdc42. Cell **102:**325–334.
13. **Gold, E. S., N. S. Morrissette, D. M. Underhill, J. Guo, M. Bassetti, and A. Aderem.** 2000. Amphiphysin IIm, a novel amphiphysin II isoform, is required for macrophage phagocytosis. Immunity **12:**285–292.
14. **Gold, E. S., D. M. Underhill, N. S. Morrissette, J. Guo, M. A. McNiven, and A. Aderem.** 1999. Dynamin 2 is required for phagocytosis in macrophages. J. Exp. Med. **190:**1849–1856.
15. **Grabs, D., V. I. Slepnev, Z. Songyang, C. David, M. Lynch, L. C. Cantley, and P. De Camilli.** 1997. The SH3 domain of amphiphysin binds the proline-rich domain of dynamin at a single site that defines a new SH3 binding consensus sequence. J. Biol. Chem. **272:**13419–13425.
16. **Greber, U. F.** 2002. Signalling in viral entry. Cell Mol. Life Sci. **59:**608–626.
17. **Greber, U. F.** 1998. Virus assembly and disassembly: the adenovirus cysteine protease as a trigger factor. Rev. Med. Virol. **8:**213–222.
18. **Greber, U. F., P. Webster, J. Weber, and A. Helenius.** 1996. The role of the adenovirus protease in virus entry into cells. EMBO J. **15:**1766–1777.
19. **Greber, U. F., M. Willetts, P. Webster, and A. Helenius.** 1993. Stepwise dismantling of adenovirus 2 during entry into cells. Cell **75:**477–486.
20. **Gruenberg, J.** 2001. The endocytic pathway: a mosaic of domains. Nat. Rev. Mol. Cell. Biol. **2:**721–730.
21. **Gu, H., R. J. Botelho, M. Yu, S. Grinstein, and B. G. Neel.** 2003. Critical role for scaffolding adapter Gab2 in Fc gamma R-mediated phagocytosis. J. Cell Biol. **161:**1151–1161.
22. **Guermonprez, P., L. Saveanu, M. Kleijmeer, J. Davoust, P. Van Endert, and S. Amigorena.** 2003. ER-phagosome fusion defines an MHC class I cross-presentation compartment in dendritic cells. Nature **425:**397–402.
23. **Halstead, S. B.** 1994. Antibody-dependent enhancement of infection: a mechanism for indirect virus entry into cells, p. 493–516. *In* E. Wimmer (ed.), Cellular receptors for animal viruses. Cold Spring Harbor Laboratory Press, Cold Spring Harbor, N.Y.
24. **Heukeshoven, J., and R. Dernick.** 1988. Improved silver staining procedure for fast staining in PhastSystem development unit. I. Staining of sodium dodecyl sulfate gels. Electrophoresis **9:**28–32.
25. **Hewlett, L. J., A. R. Prescott, and C. Watts.** 1994. The coated pit and macropinocytic pathways serve distinct endosome populations. J. Cell Biol. **124:**689–703.
26. **Hinrichsen, L., J. Harborth, L. Andrees, K. Weber, and E. J. Ungewickell.** 2003. Effect of clathrin heavy chain- and alpha-adaptin-specific small inhibitory RNAs on endocytic accessory proteins and receptor trafficking in HeLa cells. J. Biol. Chem. **278:**45160–45170.
27. **Houde, M., S. Bertholet, E. Gagnon, S. Brunet, G. Goyette, A. Laplante, M. F. Princiotta, P. Thibault, D. Sacks, and M. Desjardins.** 2003. Phagosomes are competent organelles for antigen cross-presentation. Nature **425:** 402–406.
28. **Johannes, L., and C. Lamaze.** 2002. Clathrin-dependent or not: is it still the question? Traffic **3:**443–451.
29. **Lavillette, D., S. J. Russell, and F. L. Cosset.** 2001. Retargeting gene delivery using surface-engineered retroviral vector particles. Curr. Opin. Biotechnol. **12:**461–466.
30. **Mabit, H., M. Y. Nakano, U. Prank, B. Saam, K. Döhner, B. Sodeik, and U. F. Greber.** 2002. Intact microtubules support adenovirus and herpes simplex virus infections. J. Virol. **76:**9962–9971.
31. **Maniak, M.** 2002. Conserved features of endocytosis in Dictyostelium. Int. Rev. Cytol. **221:**257–287.
32. **Marini, F. C., III, Q. Yu, T. Wickham, I. Kovesdi, and M. Andreeff.** 2000. Adenovirus as a gene therapy vector for hematopoietic cells. Cancer Gene Ther. **7:**816–825.
33. **Marsh, M., and H. T. McMahon.** 1999. The structural era of endocytosis. Science **285:**215–220.
34. **Maxfield, F. R., and T. E. McGraw.** 2004. Endocytic recycling. Nat. Rev. Mol. Cell Biol. **5:**121–132.
35. **Meier, O., K. Boucke, S. Vig, S. Keller, R. P. Stidwill, S. Hemmi, and U. F. Greber.** 2002. Adenovirus triggers macropinocytosis and endosomal leakage together with its clathrin mediated uptake. J. Cell Biol. **158:**1119–1131.
36. **Meier, O., and U. F. Greber.** 2003. Adenovirus endocytosis. J. Gene Med. **5:**451–462.

37. **Mercier, S., H. Rouard, M. H. Delfau-Larue, and M. Eloit.** 2004. Specific antibodies modulate the interactions of adenovirus type 5 with dendritic cells. Virology **322:**308–317.
38. **Morgan, J. R., K. Prasad, S. Jin, G. J. Augustine, and E. M. Lafer.** 2003. Eps15 homology domain-NPF motif interactions regulate clathrin coat assembly during synaptic vesicle recycling. J. Biol. Chem. **278:**33583–33592.
39. **Moron, V. G., P. Rueda, C. Sedlik, and C. Leclerc.** 2003. In vivo, dendritic cells can cross-present virus-like particles using an endosome-to-cytosol pathway. J. Immunol. **171:**2242–2250.
40. **Motley, A., N. A. Bright, M. N. Seaman, and M. S. Robinson.** 2003. Clathrin-mediated endocytosis in AP-2-depleted cells. J. Cell Biol. **162:**909–918.
41. **Mukherjee, S., R. N. Ghosh, and F. R. Maxfield.** 1997. Endocytosis. Physiol. Rev. **77:**759–803.
42. **Nagel, H., S. Maag, A. Tassis, F. O. Nestle, U. F. Greber, and S. Hemmi.** 2003. The alphavbeta5 integrin of hematopoietic and nonhematopoietic cells is a transduction receptor of RGD-4C fiber-modified adenoviruses. Gene Ther. **10:**1643–1653.
43. **Nakano, M. Y., K. Boucke, M. Suomalainen, R. P. Stidwill, and U. F. Greber.** 2000. The first step of adenovirus type 2 disassembly occurs at the cell surface, independently of endocytosis and escape to the cytosol. J. Virol. **74:**7085–7095.
44. **Nichols, B. J., and J. Lippincott-Schwartz.** 2001. Endocytosis without clathrin coats. Trends Cell Biol. **11:**406–412.
45. **Nobes, C., and M. Marsh.** 2000. Dendritic cells: new roles for Cdc42 and Rac in antigen uptake? Curr. Biol. **10:**R739–R741.
46. **Norbury, C. C., B. J. Chambers, A. R. Prescott, H. G. Ljunggren, and C. Watts.** 1997. Constitutive macropinocytosis allows TAP-dependent major histocompatibility complex class I presentation of exogenous soluble antigen by bone marrow-derived dendritic cells. Eur. J. Immunol. **27:**280–288.
47. **Owen, D. J., P. Wigge, Y. Vallis, J. D. Moore, P. R. Evans, and H. T. McMahon.** 1998. Crystal structure of the amphiphysin-2 SH3 domain and its role in the prevention of dynamin ring formation. EMBO J. **17:**5273–5285.
48. **Pelkmans, L., and A. Helenius.** 2003. Insider information: what viruses tell us about endocytosis. Curr. Opin. Cell Biol. **15:**414–422.
49. **Perry, D. G., G. L. Daugherty, and W. J. Martin II.** 1999. Clathrin-coated pit-associated proteins are required for alveolar macrophage phagocytosis. J. Immunol. **162:**380–386.
50. **Poranen, M. M., R. Daugelavicius, and D. H. Bamford.** 2002. Common principles in viral entry. Annu. Rev. Microbiol. **56:**521–538.
51. **Robinson, M. S.** 2004. Adaptable adaptors for coated vesicles. Trends Cell Biol. **14:**167–174.
52. **Shupliakov, O., P. Low, D. Grabs, H. Gad, H. Chen, C. David, K. Takei, P. De Camilli, and L. Brodin.** 1997. Synaptic vesicle endocytosis impaired by disruption of dynamin-SH3 domain interactions. Science **276:**259–263.
53. **Sirena, D., B. Lilienfeld, M. Eisenhut, S. Kaelin, K. Boucke, R. R. Beerli, L. Vogt, C. Ruedl, M. F. Bachmann, U. F. Greber, and S. Hemmi.** 2004. The human membrane cofactor CD46 is a receptor for species B adenovirus serotype 3. J. Virol. **78:**4454–4462.
54. **Slepnev, V. I., G. C. Ochoa, M. H. Butler, and P. De Camilli.** 2000. Tandem arrangement of the clathrin and AP-2 binding domains in amphiphysin 1 and disruption of clathrin coat function by amphiphysin fragments comprising these sites. J. Biol. Chem. **275:**17583–17589.
55. **Swanson, J. A., and C. Watts.** 1995. Macropinocytosis. Trends Cell Biol. **5:**424–428.
56. **Tse, S. M., W. Furuya, E. Gold, A. D. Schreiber, K. Sandvig, R. D. Inman, and S. Grinstein.** 2003. Differential role of actin, clathrin, and dynamin in Fc gamma receptor-mediated endocytosis and phagocytosis. J. Biol. Chem. **278:**3331–3338.
57. **Van de Winkel, J. G., and P. J. Capel.** 1993. Human IgG Fc receptor heterogeneity: molecular aspects and clinical implications. Immunol. Today **14:**215–221.
58. **van Raaij, M. J., E. Chouin, H. van der Zandt, J. M. Bergelson, and S. Cusack.** 2000. Dimeric structure of the coxsackievirus and adenovirus receptor D1 domain at 1.7 A resolution. Struct. Fold Des. **8:**1147–1155.
59. **Wang, K., S. Huang, A. Kapoor-Munshi, and G. Nemerow.** 1998. Adenovirus internalization and infection require dynamin. J. Virol. **72:**3455–3458.
60. **West, M. A., A. R. Prescott, E. L. Eskelinen, A. J. Ridley, and C. Watts.** 2000. Rac is required for constitutive macropinocytosis by dendritic cells but does not control its downregulation. Curr. Biol. **10:**839–848.
61. **Wickham, T. J.** 2003. Ligand-directed targeting of genes to the site of disease. Nat. Med. **9:**135–139.
62. **Wickham, T. J., P. Mathias, D. A. Cheresh, and G. R. Nemerow.** 1993. Integrins alpha v beta 3 and alpha v beta 5 promote adenovirus internalization but not virus attachment. Cell **73:**309–319.
63. **Wilson, B. S., J. R. Pfeiffer, and J. M. Oliver.** 2000. Observing FcepsilonRI signaling from the inside of the mast cell membrane. J. Cell Biol. **149:**1131–1142.
64. **Woof, J. M., and D. R. Burton.** 2004. Human antibody-Fc receptor interactions illuminated by crystal structures. Nat. Rev. Immunol. **4:**89–99.
65. **Xia, H., B. Anderson, Q. Mao, and B. L. Davidson.** 2000. Recombinant human adenovirus: targeting to the human transferrin receptor improves gene transfer to brain microcapillary endothelium. J. Virol. **74:**11359–11366.
66. **Zerial, M., and H. McBride.** 2001. Rab proteins as membrane organizers. Nat. Rev. Mol. Cell Biol. **2:**107–117.